

Published in final edited form as:

*Biochemistry*. 2011 November 29; 50(47): 10399–10407. doi:10.1021/bi201126r.

## Preparation of an Activated Rhodopsin/Transducin Complex Using a Constitutively Active Mutant of Rhodopsin

Guifu Xie<sup>‡</sup>, Aaron M. D'Antona<sup>‡</sup>, Patricia C. Edwards<sup>§</sup>, Maikel Fransen<sup>§</sup>, Jorg Standfuss<sup>#</sup>, Gebhard F. X. Schertler<sup>#,\*</sup>, and Daniel D. Oprian<sup>‡,\*</sup>

<sup>‡</sup>Department of Biochemistry, Brandeis University, Waltham, Massachusetts 02454 <sup>§</sup>MRC Laboratory of Molecular Biology, Hills Road, Cambridge CB2 0QH, UK <sup>#</sup>Paul Scherrer Institut, Villigen PSI, 5232, Switzerland

### Abstract

The interaction of rhodopsin and transducin has been the focus of study for more than 30 years, but only recently have efforts to purify an activated complex in detergent solution materialized. These efforts have used native rhodopsin isolated from bovine retina and employed either sucrose density gradient centrifugation or size exclusion chromatography to purify the complex. While there is general agreement on most properties of the activated complex, subunit stoichiometry is not yet settled, with rhodopsin/transducin molar ratios of both 2/1 and 1/1 reported. In this report, we introduce methods for preparation of the complex that include use of recombinant rhodopsin, so as to take advantage of mutations that confer constitutive activity and enhanced thermal stability on the protein, and immunoaffinity chromatography for purification of the complex. We show that chromatography on ConA-Sepharose can substitute for the immunoaffinity column, and that bicelles can be used instead of detergent solution. We demonstrate the following: that rhodopsin has a covalently bound all-*trans*-retinal chromophore and therefore corresponds to the active metarhodopsin II state; that transducin has an empty nucleotide-binding pocket; that the isolated complex is active and dissociates upon addition of guanine nucleotide; and finally that the stoichiometry corresponds reproducibly to a 1/1 molar ratio of rhodopsin to transducin.

Rhodopsin is the visual pigment of vertebrate rod photoreceptor cells and a prototypical member of the large class of G protein-coupled receptors (1–4). It is composed of an apoprotein, opsin, and a covalently bound 11-*cis*-retinal chromophore. Upon absorption of light, the chromophore undergoes isomerization to the all-*trans*-form resulting in a cascade of reactions that result ultimately in closure of cGMP-gated cation channels in the rod outer segment, hyperpolarization of the plasma membrane, and inhibition of glutamate release from the synaptic terminus of the rod cell. The cascade is initiated by a conformational change in rhodopsin that is triggered by isomerization of the chromophore and leads to activation of the G protein transducin. Indeed, activation of a G protein is the signature response of activated G protein-coupled receptors from which this family of receptors derives its name (2).

Crystal structures have been determined for the inactive and active states of several GPCRs (5–22), including a number for rhodopsin bound to a peptide from the carboxy-terminus of

\*To whom correspondence should be addressed: D.D.O., oprian@brandeis.edu; G.F.X.S., gebhard.schertler@psi.ch. Contact D.D.O. via phone at (617) 736-2322.

<sup>1</sup>Abbreviations: BSA, bovine serum albumin; DDM, Dodecyl β-D-maltoside; DHPC 1,2-diheptanoyl-*sn*-glycero-3-phosphocholine; DMEM, Dulbecco's modified Eagle's medium; DMPC, 1,2-Dimyristoyl-*sn*-glycero-3-phosphocholine; DTT, dithiothreitol; BGS, bovine growth serum; PBS, phosphate buffered saline; ROS, rod outer segments.

the alpha subunit of transducin (23–26), but it is generally recognized that a complete understanding of the activation process will require a structure of an activated complex of receptor and intact G protein, a goal that has been described as “The Holy Grail” for the field (27).

While the biochemical literature on activation of transducin by rhodopsin is rich and dates back thirty years (28), efforts at purification of an activated complex of the two proteins have been reported only recently (29–33). These efforts have generally employed size-exclusion chromatography (30) or sucrose-density gradient centrifugation (31, 32) to purify the complex, and have uniformly used native rhodopsin because of its ready availability in large quantity from commercial sources and ease of purification.

We report here the purification and characterization of an activated complex of rhodopsin and transducin using a constitutively active mutant of rhodopsin (34) known for slow decay of the active metarhodopsin II state (35, 36) in combination with an engineered disulfide bond known to enhance thermal stability of rhodopsin in detergent solution (18, 37). Purification of the complex exploits an immunoaffinity procedure originally developed for purification of rhodopsin heterologously expressed from transfected mammalian cells in culture (37, 38). We show that the complex forms only if rhodopsin is in the activated state, that the nucleotide-binding site in transducin is empty, and that the molar ratio of rhodopsin to transducin in the complex is 1/1. Finally, we show that the complex can be prepared using bicelles (39, 40) instead of detergent solubilized proteins.

## EXPERIMENTAL PROCEDURES

### Materials

11-*cis*- and all-*trans*-Retinal were synthesized according to published procedures and purified first by chromatography on silica gel (70–230 mesh from Aldrich) using a 15% ether/85% hexane mixture, and then by crystallization from petroleum ether, as has been described (37). 1,2-Dimyristoyl-*sn*-glycero-3-phosphocholine (DMPC) and 1,2-diheptanoyl-*sn*-glycero-3-phosphocholine (DHPC) were from Avanti Polar Lipids, Inc. (Alabaster, AL). Dodecyl  $\beta$ -D-maltoside (DDM) was purchased from Calbiochem (La Jolla, CA), Dulbecco's modified Eagle's medium (DMEM) was from GIBCO (Carlsbad, CA), and bovine growth serum (BGS) and Dulbecco's phosphate buffered saline (PBS) from Hyclone Laboratories, Inc. (Logan, UT). Concanavalin A-Sepharose 4B (ConA-Sepharose) was a product of Sigma-Aldrich (St. Louis, MO). [<sup>35</sup>S]-GTP $\gamma$ S (1250 Ci/mmol) and [ $\alpha$ -<sup>32</sup>P]-GTP (3000 Ci/mmol) were from Perkin Elmer (Boston, MA); nonradiolabeled GTP and GTP $\gamma$ S were from Amersham Biosciences (Piscataway, NJ) and Sigma-Aldrich (St. Louis, MO), respectively.

The anti-rhodopsin monoclonal antibody 1D4 (41, 42) was from the National Cell Culture Center (Minneapolis, MN). The 1D4-Sepharose 4B immunoaffinity matrix (1D4-Sepharose) used for purification of rhodopsin and the rhodopsin/transducin complex was prepared as previously described (38). 1D4-peptide, a synthetic peptide corresponding to the carboxy-terminal 8 amino acids of rhodopsin and epitope for the 1D4-antibody (ETSQVAPA), was used for elution of rhodopsin (and the activated rhodopsin/transducin complex) from the 1D4-Sepharose matrix (38).

Transducin was purified from bovine retinae essentially as described previously (43). Frozen bovine retinae, purchased from Schenk Packing Co., Inc. (Stanwood, WA), were used to prepare rod photoreceptor cell outer segments (ROS). Following isotonic and hypotonic washes, 40  $\mu$ M GTP was added to release transducin from the purified ROS membranes. Transducin was then separated from ROS by centrifugation, filtered through a 0.22  $\mu$ m membrane (Steriflip from Millipore Corp., Billerica, MA), concentrated, and dialyzed

against 10 mM Tris buffer, pH 7.4, containing 2 mM MgCl<sub>2</sub>, 1 mM DTT, and 50% glycerol for storage at -20°C before use. Transducin concentration was determined by active-site titration with radiolabeled [<sup>35</sup>S]-GTPγS of known specific radioactivity, and was typically within 5–10% of the value determined by Lowry assay (44) using BSA as a standard. The same purification procedure was followed for preparation of transducin containing [α-<sup>32</sup>P]-GDP in the nucleotide binding site except that 40 μM [α-<sup>32</sup>P]-GTP (0.31 Ci/mmol) was used instead of nonradiolabeled GTP for release of transducin from ROS membranes.

### Expression of Rhodopsin in HEK293 Cells

With the exception of Figure 8, all experiments in this study were conducted with the N2C,E113Q,D282C triple mutant of rhodopsin. This mutant combines the constitutive activity of the E113Q mutant (34) with the increased thermal stability of the N2C,D282C mutant (37). The N2C,E113Q,D282C mutant was expressed transiently in HEK293S-GnT1<sup>-</sup> cells (45) following transfection using calcium phosphate precipitation. Cells were harvested 72 hr post-transfection and solubilized with 1% (w/v) DDM in PBS (10 mM sodium phosphate buffer, pH 7.5, containing 150 mM NaCl) and 0.2 mg/ml phenylmethylsulfonyl fluoride at 4°C for 1 hr, essentially as described previously for expression of rhodopsin in COS cells (37, 38).

### Purification of Rhodopsin From HEK293 Cells

Nuclei were removed from detergent solubilized HEK293 cells by centrifugation for 5 min at 1200g. The mutant opsin was then purified from the supernate by immunoaffinity chromatography on 1D4-Sepharose 4B (37, 38). Opsin was allowed to bind to the resin overnight at 4°C. The 1D4-Sepharose was then washed with 0.1% DDM in PBS, chromophore (11-*cis* or all-*trans* retinal) was added in PBS containing 0.1% DDM (1 hr incubation), and the resin washed again with Buffer A (5 mM Hepes buffer, pH 7.5, and 0.1 mM MgCl<sub>2</sub>) containing 0.02% DDM at 4°C to remove free retinal and lower the salt concentration. Rhodopsin was eluted from the resin following incubation at room temperature for 30 min in Buffer A containing 80 μM 1D4 peptide.

Purification of the mutant pigments using ConA-Sepharose chromatography was performed in a similar manner except that bound protein was eluted with 200 mM methyl α-D-mannoside in 0.02% DDM, 20 mM Hepes, pH 7.5, 0.1 mM MgCl<sub>2</sub> and 120 mM NaCl.

### Preparation and Purification of Activated Rhodopsin/Transducin Complexes

Purification of the activated complexes was performed according to the same protocols used for purification of rhodopsin from transfected cells with modification as indicated in Results.

### Complex Stoichiometry

The relative stoichiometry of rhodopsin and transducin in the activated complex was determined by densitometry of protein bands following electrophoretic separation on SDS-PAGE gels. Purified complex was visualized by staining with Coomassie Blue. Band densities of the purified complex proteins were quantified from background-subtracted band intensities of digitized gel images using ImageJ version 1.38 software (W.S. Rasband, NIH, <http://rsbweb.nih.gov/ij/>, 1997-2007) using a standard curve of known amounts of transducin and rhodopsin.

### Preparation and Purification of the Rhodopsin/Transducin Complex in Bicelles

Stock DMPC/DHPC bicelle solutions at 20% (w/v, total lipid; [DMPC]/[DHPC] = 0.65) were prepared by first removing chloroform from the phospholipid stocks by drying under N<sub>2</sub> and then under vacuum for at least two hours, and resuspending the powder in Buffer A.

The DMPC/DHPC mixture was repeatedly vortexed, heated to 42 °C for 15 min, and placed on ice for 30 min until the lipids were in solution. Bicelles were stored at 4 °C and used within 24 h.

Isolation of the rhodopsin/transducin complex in DMPC/DHPC bicelles was performed by first immobilizing complexes on 1D4-Sepharose 4B in Buffer A containing 0.02% DDM. The bound complexes were then washed extensively with 2.5% (w/v, total lipid) DMPC/DHPC bicelle solution in Buffer A. 80  $\mu\text{M}$  1D4-peptide or 40  $\mu\text{M}$  GTP $\gamma\text{S}$  in Buffer A containing 2.5% DMPC/DHPC was used to elute bound protein from the affinity resin at room temperature.

### Transducin Activation Assays

The ability of rhodopsin to catalyze the light-dependent exchange of radiolabeled [ $^{35}\text{S}$ ]-GTP $\gamma\text{S}$  for bound GDP in transducin was monitored using a filter-binding assay as has been described previously (46). To assay the rhodopsin/transducin complex for activity, a similar procedure was used except that the purified complex was diluted to a final concentration of 30 to 40 nM rhodopsin in the reaction mixture consisting of 10 mM Tris buffer, pH 7.5, 0.1% (w/v) DDM, 5 mM  $\text{MgCl}_2$ , and 1 mM DTT but no additional transducin. Reactions were initiated by addition of 40  $\mu\text{M}$  [ $^{35}\text{S}$ ]-GTP $\gamma\text{S}$  (1.42 Ci/mmol) and then incubated for 5 min at 25°C before aliquots were withdrawn and applied to filters.

### Absorption Spectroscopy

UV-visible absorption spectra were recorded using a Hitachi model U-3210 spectrophotometer that was specifically modified by the manufacturer for use in a darkroom. Data were collected with a microcomputer using GraphPad Prism (GraphPad Software, San Diego, CA). All samples were recorded at 25°C with a path length of 1.0 cm. The absorption coefficient for the rhodopsin mutant was determined by acid-trapping of the chromophore essentially as has been described for the human blue color vision pigment (47) except that 50 mM sodium phosphate buffer, pH 3.5, containing 0.5% (w/v) SDS was used instead of HCl to denature the protein and trap the chromophore. The molar extinction coefficient,  $\epsilon_{380}$ , for  $\text{Gt}_{\text{empty}}$  was determined to be 87,800  $\text{M}^{-1} \text{cm}^{-1}$  using the Edelhoch method (48) with the extinction coefficients for Trp and Tyr (49).  $\text{GTP } \epsilon_{280} = 5,770 \text{ M}^{-1} \text{cm}^{-1}$  was derived from the known  $\epsilon_{253} = 13,700 \text{ M}^{-1} \text{cm}^{-1}$  and was used to calculate  $\epsilon_{280}$  for  $\text{Gt}_{\text{GDP}} = 93,570 \text{ M}^{-1} \text{cm}^{-1}$ .

## RESULTS

### Activation of Transducin in the Presence of the 1D4-Antibody

Our strategy to form and purify the activated rhodopsin/transducin complex exploits the procedure for immunoaffinity purification of rhodopsin from low-abundance sources (such as heterologous expression systems) using the 1D4-antibody immobilized on Sepharose 4B (37, 38). This approach takes advantage of the tight binding interaction between metarhodopsin II and transducin, and the specific interaction of the 1D4-antibody with rhodopsin. We were concerned initially that immobilization of rhodopsin on the antibody column might interfere with formation of the complex because both the transducin binding site and 1D4-epitope are located on the cytoplasmic surface of rhodopsin. However, as is shown in Figure 1, the ability of rhodopsin to activate transducin is unaffected by the presence of the 1D4-antibody at concentrations up to 1  $\mu\text{M}$ . Under these conditions, >95% of the rhodopsin is expected to be in complex with the antibody (50). Therefore, it is clear that binding of the 1D4-antibody to rhodopsin does not inhibit the ability of rhodopsin to catalyze the light-dependent activation of transducin. While surprising, this conclusion is supported by the fact (presented below) that an activated complex of rhodopsin and

transducin can be purified by immunoaffinity chromatography on 1D4-Sepahrose. A highly similar complex (also presented below) can be purified by chromatography on ConA-Sepahrose (which targets rhodopsin's oligosaccharyl chain on the extracellular surface of the protein).

### Purification and Characterization of the Activated Rhodopsin/Transducin Complex

The activated rhodopsin/transducin complex was prepared by first solubilizing HEK293S-GnTI<sup>-</sup> cells expressing the N2C,E113Q,D282C triple mutant opsin in 1% DDM (w/v), centrifuging the material at low speed to remove nuclei, and applying the post-nuclear supernatant fraction to a 1D4-Sepahrose antibody immunoaffinity matrix. The immobilized triple mutant opsin was then reconstituted with all-*trans*-retinal while still bound to the column, and excess transducin (typically 1.5–2 times the amount of rhodopsin) was added (Figure 2A, *lane 1*). The unbound fraction (Figure 2A, *lane 2*) contained visibly less transducin than was applied to the column, and typically also contained small amounts of rhodopsin released during the transducin-binding step (this shedding of rhodopsin from the column also takes place in the absence of complex formation; see Figure 5, *lane 7* below). After extensive washing of the column (Figure 2, *lane 3*), rhodopsin and transducin were both released from the immunoaffinity matrix by incubation with the 1D4-peptide in 0.02% (w/v) DDM (Figure 2, *lane 4*). In separate control experiments not shown, transducin alone did not bind to the 1D4-Sepahrose matrix. We conclude that transducin binds to the immobilized N2C,E113Q,D282C mutant, and that both are released as a complex by incubation with the 1D4-peptide.

Absorption spectra for the N2C,E113Q,D282C mutant purified in the presence or absence of transducin are shown in Figure 2B. Both spectra show an absorption maximum ( $\lambda_{\max}$ ) at 380 nm, characteristic of the unprotonated Schiff base form of the all-*trans*-retinal chromophore, as well as a second  $\lambda_{\max}$  at 280 nm characteristic of protein. It is noteworthy that there is far more absorbance at 280 nm when the mutant is purified in the presence of transducin (*spectrum 1*) than in its absence (*spectrum 2*), indicating the presence of co-purified transducin in the former sample.

The absorption coefficient at 380 nm for the triple mutant rhodopsin in the activated complex was determined by acid denaturation in SDS solution, as has been described previously (47). When a purified sample of the complex in 5 mM HEPES buffer, pH 7.5, containing 0.1 mM MgCl<sub>2</sub> and 0.02% (w/v) DDM (Figure 3, *spectrum 1*) was denatured by addition of 50 mM sodium phosphate, pH 3.5, and 0.5% SDS, the 380-nm peak was converted to a new  $\lambda_{\max}$  at 440 nm (*spectrum 2*) characteristic of a protonated retinylidene Schiff base, with little change in absorbance at 280 nm. The absence of a residual 380-nm peak under acid conditions suggests that most of the retinal was covalently bound to protein, and little remained free in the sample. The absorption coefficient at 380 nm ( $\epsilon_{380}$ ) for the all-*trans*-retinal chromophore in the rhodopsin/transducin complex (Figure 3, *spectrum 1*) was calculated from the data of Figure 3 to be 42,600 M<sup>-1</sup>cm<sup>-1</sup>, using the acid denatured form of native metarhodopsin II as a standard for the absorption coefficient of the 440-nm species (Figure 3, *Spectrum 2*).

The  $\epsilon_{380}$  for the rhodopsin/transducin complex determined from Figure 3 was then used with the spectra of Figure 2B to make an initial, rough estimation of protein subunit stoichiometry in the complex as follows. The  $\epsilon_{380}$  for rhodopsin from Figure 3 is 42,600 M<sup>-1</sup>cm<sup>-1</sup>. The  $\epsilon_{280}$  for rhodopsin was determined from the  $\epsilon_{380}$  and *spectrum 2* of Figure 2 to be 68,160 M<sup>-1</sup>cm<sup>-1</sup> (i.e.,  $\epsilon_{280} = 1.6 \times 42,600$ ). The  $\epsilon_{280}$  for the nucleotide-free form of transducin in the complex (see below) was calculated from the known amino acid sequence of the protein to be 87,800 M<sup>-1</sup>cm<sup>-1</sup>. Finally, the ratio of absorbance at 280 nm to that at 380 nm ( $A_{280 \text{ nm}}/A_{380 \text{ nm}}$ ) for a 1/1 complex of activated rhodopsin and transducin was



calculated from the absorption coefficients to be 3.7  $((68,160 + 87,800)/42,600)$ . The actual  $A_{280\text{ nm}}/A_{380\text{ nm}}$  measured from Figure 2 for the purified complex is 3.7, a figure in much better agreement with that expected for a complex with 1/1 stoichiometry (Rho/Gt) than either a 2/1 complex (2.6) or a 1/2 complex (5.7).

To address concerns that the 1D4-antibody, which recognizes an epitope located on the same face of rhodopsin as the transducin binding site, may influence subunit stoichiometry in the complex, an alternate purification strategy was employed using ConA-Sepharose. ConA, like the 1D4-antibody, targets structural determinants on rhodopsin, but these are the carbohydrate moieties located on the extracellular side of the membrane, opposite the transducin binding site. Except for the exchange of affinity support and associated eluant, all other steps in the purification protocol were identical to those employed using 1D4-Sepharose. As can be seen in a comparison of Figure 4, *lane 4* with Figure 2, *lane 4*, a very similar complex (with similar yield) was obtained using ConA-Sepharose as a replacement for the 1D4-Sepharose affinity matrix ( $A_{280\text{ nm}}/A_{380\text{ nm}} = 3.6$ ; data not shown). Therefore, we conclude that the use of the 1D4-antibody does not influence subunit stoichiometry in the activated complex.

An additional determination of subunit stoichiometry was performed for the complex by measuring directly the nucleotide-binding capacity of transducin in the purified complex. Samples of complex purified on 1D4-Sepharose were diluted into a reaction mixture containing 40  $\mu\text{M}$  [ $^{35}\text{S}$ ]-GTP $\gamma\text{S}$ , and bound nucleotide was determined using a standard filter-binding assay and scintillation counting. The ratio of transducin, as determined by bound [ $^{35}\text{S}$ ]-GTP $\gamma\text{S}$ , to rhodopsin, as determined by  $A_{380\text{ nm}}$ , was typically one mole of transducin per mole of triple mutant (Gt/Rho =  $0.89 \pm 0.06$ ,  $n = 6$ ; data not shown).

### Dependence on Activated State of Rhodopsin

As can be seen in Figure 5, the rhodopsin/transducin complex did not form when 11-*cis*-retinal replaced the all-*trans*-isomer and purification was carried out in the dark. Binding of 11-*cis*-retinal forces the protein into the inactive state and disrupts the interaction with transducin. Thus, only rhodopsin is eluted from the 1D4-Sepharose matrix with 1D4-peptide when purification is performed in the dark with 11-*cis*-retinal (Figure 5A, *lane 9*); the GTP $\gamma\text{S}$  eluate is also free of transducin (Figure 5A, *lane 10*). The absorption spectrum for the sample in Fig. 5A, *lane 9* displayed an  $A_{280\text{ nm}}/A_{380\text{ nm}}$  ratio of 1.7 (Figure 5B, *spectrum 2*), as expected for pure rhodopsin and in agreement with the data in Figure 5A suggesting that transducin does not copurify with rhodopsin under these conditions. Therefore, formation of the rhodopsin/transducin complex requires rhodopsin to be in the activated state.

A final determination of subunit stoichiometry in the purified complex was determined by densitometry of band intensities following separation by SDS-PAGE as is shown in Figure 6. Gels containing samples of purified complex from the 1D4-support and known standards for transducin and the rhodopsin mutant were scanned, and bands in the digitized images integrated. As can be seen in Figure 6, the data are in support of a 1/1 complex of transducin and activated rhodopsin.

### Nucleotide-Binding State of Transducin in the Complex

It is well established that rhodopsin catalyzes GDP release from  $\text{G}\alpha$  in the initial steps of formation of the rhodopsin-transducin complex. To test whether nucleotide was released, transducin containing [ $\alpha$ - $^{32}\text{P}$ ]-GDP of known specific activity in the nucleotide-binding pocket was used to form the activated complex. As is shown in Figure 7, no radioactivity was associated with the complex following elution from the 1D4-immunoaffinity matrix

with 1D4-peptide while both transducin and rhodopsin were clearly present, as judged by SDS-PAGE. Therefore, transducin must contain an empty nucleotide-binding pocket in the activated complex.

### Formation of the Complex Using Light-Activated Wild-Type Rhodopsin

To eliminate concern that the 1/1 stoichiometry in the complex was somehow a consequence of using a constitutively active mutant of rhodopsin, we repeated the procedure using light-activated native rhodopsin purified from bovine retina (Fig. 8A) and recombinant N2C,D282C rhodopsin from HEK293 cells (Fig. 8B) to form the complex (both containing 11-cis-retinal before exposure to light). As is shown in Figure 8, SDS-PAGE of the complexes in each case showed similar subunit composition to that found with the N2C,E113Q,D282C mutant (compare with Fig. 2A), and quantification using the [<sup>35</sup>S]-GTPγS filter binding assay showed rhodopsin and transducin were present in 1/1 molar ratio (not shown).

### Purification of the Complex in Phospholipid Bicelles

Isolation of the activated rhodopsin/transducin complex in DMPC/DHPC bicelles was performed by first immobilizing the N2C,E113Q,D282C opsin on 1D4-Sepharose in 1% DDM. The protein was then reconstituted with all-*trans*-retinal and incubated with a 2-fold excess of transducin in PBS containing 0.1% DDM. The bound complex was then washed in 0.02% DDM, followed by extensive washing with 2.5% DMPC/DHPC (w/v, total lipid; [DMPC]/[DHPC] = 0.65) bicelle solution in Buffer A. The activated complex eluted with 1D4-peptide in the same solution (Figure 9, *lane 4*) appears similar to that obtained in detergent solution (Figure 2A, *lane 4*), although careful determination of stoichiometry was not performed for the complex in bicelles. Only transducin was released from the affinity matrix when the eluant was GTPγS in Buffer A containing 2.5% DMPC/DHPC bicelles (Figure 9, *lane 5*).

## DISCUSSION

Pioneering studies in the early 1980s by Kuhn, Chabre, and Hofmann established key characteristics of an activated complex of rhodopsin and the G protein transducin using rod photoreceptor cell disk membranes. In particular, Emeis et al. (51) demonstrated that transducin binds preferentially to the metarhodopsin II intermediate and is able to shift the MI-MII equilibrium in an assay that has since been referred to as “extra-meta II”; Bornancin et al. (52) established that the activated complex, designated R<sub>ret</sub>\*-T<sub>e</sub>, is composed of rhodopsin in the metarhodopsin II state bound to transducin with an empty nucleotide binding pocket; and Kuhn et al. (53) used light-scattering changes in disk membranes to establish a molar stoichiometry for the complex of 1 rhodopsin to 1 transducin. In addition, Kuhn (54) made an early attempt at isolation of a rhodopsin/transducin complex in soluble form by immobilizing rhodopsin on a ConA-Sepharose column in detergent solution. While he did not purify the complex, he did show that transducin bound to the column and could be specifically eluted by addition of GTPγS (54).

More recently several groups have undertaken purification of the complex in detergent solution (30–33). These efforts have used native rhodopsin isolated from bovine retina exclusively and employed sucrose density gradient centrifugation or size exclusion chromatography to separate the activated complex from unbound material. While there is general agreement that the minimal functional unit in transducin activation assays is a rhodopsin monomer (29, 30, 55, 56), there is not yet a consensus on subunit stoichiometry in the isolated complex; Jastrzebska et al. (31–33) find a ratio of 2 rhodopsins for each transducin whereas Ernst et al. (30) report a molar ratio of 1 rhodopsin to 1 transducin

heterotrimer in the complex. It is unclear at this time which of several differences in experimental approach might give rise to the difference in reported stoichiometries.

In the present study, we introduced two modifications in the approach to the preparation and purification of an activated complex. First, we used recombinant rhodopsin in order to take advantage of mutations in the protein that might enhance formation and stability of the activated complex. We began with the mutation E113Q (36, 57) known to slow the rate of dissociation of all-*trans*-retinal from the active metarhodopsin II state (35, 36) and confer constitutive activity on the protein (34) and placed it in the context of an engineered disulfide bond (N2C/D282C) known to enhance thermal stability of the protein in detergent solution (18, 37). Second, we used immunoaffinity chromatography with a rhodopsin-specific antibody for purification of the complex (38). We previously reported purification of an activated complex of native bovine rhodopsin and transducin in Nanodiscs using affinity chromatography on ConA-Sepharose (29). However, the use of recombinant rhodopsin in the present studies (i.e., rhodopsin from a low-abundance source) and DDM (a detergent that in our hands presents some difficulties with chromatography on ConA-Sepharose), necessitated the search for a different affinity support. To our surprise, immunoaffinity chromatography on 1D4-Sepharose worked extremely well despite the topologically juxtaposed location of the 1D4 epitope and transducin-binding site on the cytoplasmic surface of rhodopsin.

The activated complex could be formed and purified readily beginning with crude extracts from transfected HEK293 cells applied directly to the 1D4-Sepharose column. Immobilization of rhodopsin on the column was followed by incubation with the retinal chromophore and transducin to form an active complex, which could be isolated in purified form by elution from the column with the 1D4 peptide. The isolated complex displayed the expected functional characteristics. In particular, formation of the complex was absolutely dependent on the active state of rhodopsin, and all-*trans*-retinal was covalently attached to rhodopsin by means an unprotonated Schiff base. The nucleotide-binding pocket in transducin was shown to be vacant by forming the complex with G protein containing radio-labeled GDP and following loss of radioactivity from the immobilized complex. Finally, incubation with GTP $\gamma$ S caused dissociation of the complex demonstrating that the isolated complex was functionally active. We conclude that the eluted complex consists of the active species metarhodopsin II bound to the empty-pocket state of the G protein transducin.

Careful analysis of subunit stoichiometry in the isolated complex demonstrated rhodopsin and transducin to be present in a 1/1 molar ratio. This result agrees well with the stoichiometry reported by Ernst et al. (30) for the complex with native rhodopsin purified by size-exclusion chromatography in DDM solution. Importantly, we find the same stoichiometry if the complex is purified by affinity chromatography on ConA-Sepharose eliminating the possibility that the 1/1 ratio results from use of the 1D4 antibody in the purification protocol. Future efforts will target other factors that might give rise to the reported differences in subunit stoichiometry.

Recently, Kobilka and coworkers reported in a *tour de force* the crystal structure for a  $\gamma_2$ -adrenergic receptor-Gs complex (58). The complex was stabilized through interactions with a nanobody raised against the cross-linked complex, and the crystals were grown in lipidic cubic phase. Of most significance in the current context, the stoichiometry of the complex was 1 receptor to 1 G protein, in excellent agreement with the results presented here for the rhodopsin/transducin complex.

In conclusion, we have isolated an activated complex of rhodopsin and transducin by immunoaffinity chromatography in detergent solution using a constitutively active mutant of



rhodopsin. The complex contains a covalently bound all-*trans*-retinal chromophore in rhodopsin, an empty nucleotide binding pocket in transducin, is active, dissociates upon addition of guanine nucleotide, and displays a clear and reproducible 1/1 molar ratio of rhodopsin to transducin. We anticipate that this preparation may be of use in structural and mechanistic studies of signaling in the visual system.

## Acknowledgments

We thank Ben Nickle for comments on the manuscript.

This work was supported by Human Frontier Science Project (HFSP) program grant RG/0052 (D.D.O. and G.F.X.S.), The Swiss National Science Foundation (SNSF) grant 31003A\_132815/1 (J.S. and G.F.X.S.), and NIH grants T32 NS007292 and EY18542 (A.M.D.) and EY007965 (D.D.O.).

## REFERENCES

1. Hofmann KP, Scheerer P, Hildebrand PW, Choe HW, Park JH, Heck M, Ernst OP. A G protein-coupled receptor at work: the rhodopsin model. *Trends Biochem Sci.* 2009; 34:540–552. [PubMed: 19836958]
2. Rosenbaum DM, Rasmussen SG, Kobilka BK. The structure and function of G-protein-coupled receptors. *Nature.* 2009; 459:356–363. [PubMed: 19458711]
3. Smith SO. Structure and activation of the visual pigment rhodopsin. *Annu Rev Biophys.* 2010; 39:309–328. [PubMed: 20192770]
4. Kobilka B, Schertler GF. New G-protein-coupled receptor crystal structures: insights and limitations. *Trends Pharmacol Sci.* 2008; 29:79–83. [PubMed: 18194818]
5. Cherezov V, Rosenbaum DM, Hanson MA, Rasmussen SG, Thian FS, Kobilka TS, Choi HJ, Kuhn P, Weis WI, Kobilka BK, Stevens RC. High-resolution crystal structure of an engineered human beta2-adrenergic G protein-coupled receptor. *Science.* 2007; 318:1258–1265. [PubMed: 17962520]
6. Chien EY, Liu W, Zhao Q, Katritch V, Han GW, Hanson MA, Shi L, Newman AH, Javitch JA, Cherezov V, Stevens RC. Structure of the human dopamine D3 receptor in complex with a D2/D3 selective antagonist. *Science.* 2010; 330:1091–1095. [PubMed: 21097933]
7. Jaakola VP, Griffith MT, Hanson MA, Cherezov V, Chien EY, Lane JR, Ijzerman AP, Stevens RC. The 2.6 angstrom crystal structure of a human A2A adenosine receptor bound to an antagonist. *Science.* 2008; 322:1211–1217. [PubMed: 18832607]
8. Lebon G, Warne T, Edwards PC, Bennett K, Langmead CJ, Leslie AG, Tate CG. Agonist-bound adenosine A2A receptor structures reveal common features of GPCR activation. *Nature.* 2011; 474:521–525. [PubMed: 21593763]
9. Li J, Edwards PC, Burghammer M, Villa C, Schertler GF. Structure of bovine rhodopsin in a trigonal crystal form. *J Mol Biol.* 2004; 343:1409–1438. [PubMed: 15491621]
10. Murakami M, Kouyama T. Crystal structure of squid rhodopsin. *Nature.* 2008; 453:363–367. [PubMed: 18480818]
11. Nakamichi H, Okada T. Crystallographic analysis of primary visual photochemistry. *Angew Chem Int Ed Engl.* 2006; 45:4270–4273. [PubMed: 16586416]
12. Palczewski K, Kumasaka T, Hori T, Behnke CA, Motoshima H, Fox BA, Le Trong I, Teller DC, Okada T, Stenkamp RE, Yamamoto M, Miyano M. Crystal structure of rhodopsin: A G protein-coupled receptor. *Science.* 2000; 289:739–745. [PubMed: 10926528]
13. Rasmussen SG, Choi HJ, Fung JJ, Pardon E, Casarosa P, Chae PS, Devree BT, Rosenbaum DM, Thian FS, Kobilka TS, Schnapp A, Konezki I, Sunahara RK, Gellman SH, Pautsch A, Steyaert J, Weis WI, Kobilka BK. Structure of a nanobody-stabilized active state of the beta(2) adrenoceptor. *Nature.* 2011; 469:175–180. [PubMed: 21228869]
14. Rasmussen SG, Choi HJ, Rosenbaum DM, Kobilka TS, Thian FS, Edwards PC, Burghammer M, Ratnala VR, Sanishvili R, Fischetti RF, Schertler GF, Weis WI, Kobilka BK. Crystal structure of the human beta2 adrenergic G-protein-coupled receptor. *Nature.* 2007; 450:383–387. [PubMed: 17952055]

15. Rosenbaum DM, Cherezov V, Hanson MA, Rasmussen SG, Thian FS, Kobilka TS, Choi HJ, Yao XJ, Weis WI, Stevens RC, Kobilka BK. GPCR engineering yields high-resolution structural insights into beta2-adrenergic receptor function. *Science*. 2007; 318:1266–1273. [PubMed: 17962519]
16. Rosenbaum DM, Zhang C, Lyons JA, Holl R, Aragao D, Arlow DH, Rasmussen SG, Choi HJ, Devree BT, Sunahara RK, Chae PS, Gellman SH, Dror RO, Shaw DE, Weis WI, Caffrey M, Gmeiner P, Kobilka BK. Structure and function of an irreversible agonist-beta(2) adrenoceptor complex. *Nature*. 2011; 469:236–240. [PubMed: 21228876]
17. Shimamura T, Hiraki K, Takahashi N, Hori T, Ago H, Masuda K, Takio K, Ishiguro M, Miyano M. Crystal structure of squid rhodopsin with intracellularly extended cytoplasmic region. *J Biol Chem*. 2008; 283:17753–17756. [PubMed: 18463093]
18. Standfuss J, Xie G, Edwards PC, Burghammer M, Oprian DD, Schertler GF. Crystal structure of a thermally stable rhodopsin mutant. *J Mol Biol*. 2007; 372:1179–1188. [PubMed: 17825322]
19. Warne T, Moukhametzianov R, Baker JG, Nehme R, Edwards PC, Leslie AG, Schertler GF, Tate CG. The structural basis for agonist and partial agonist action on a beta(1)-adrenergic receptor. *Nature*. 2011; 469:241–244. [PubMed: 21228877]
20. Warne T, Serrano-Vega MJ, Baker JG, Moukhametzianov R, Edwards PC, Henderson R, Leslie AG, Tate CG, Schertler GF. Structure of a beta1-adrenergic G-protein-coupled receptor. *Nature*. 2008; 454:486–491. [PubMed: 18594507]
21. Wu B, Chien EY, Mol CD, Fenalti G, Liu W, Katritch V, Abagyan R, Brooun A, Wells P, Bi FC, Hamel DJ, Kuhn P, Handel TM, Cherezov V, Stevens RC. Structures of the CXCR4 chemokine GPCR with small-molecule and cyclic peptide antagonists. *Science*. 2010; 330:1066–1071. [PubMed: 20929726]
22. Xu F, Wu H, Katritch V, Han GW, Jacobson KA, Gao ZG, Cherezov V, Stevens RC. Structure of an agonist-bound human A2A adenosine receptor. *Science*. 2011; 332:322–327. [PubMed: 21393508]
23. Choe HW, Kim YJ, Park JH, Morizumi T, Pai EF, Krauss N, Hofmann KP, Scheerer P, Ernst OP. Crystal structure of metarhodopsin II. *Nature*. 2011; 471:651–655. [PubMed: 21389988]
24. Park JH, Scheerer P, Hofmann KP, Choe HW, Ernst OP. Crystal structure of the ligand-free G-protein-coupled receptor opsin. *Nature*. 2008; 454:183–187. [PubMed: 18563085]
25. Scheerer P, Park JH, Hildebrand PW, Kim YJ, Krauss N, Choe HW, Hofmann KP, Ernst OP. Crystal structure of opsin in its G-protein-interacting conformation. *Nature*. 2008; 455:497–502. [PubMed: 18818650]
26. Standfuss J, Edwards PC, D'Antona A, Fransen M, Xie G, Oprian DD, Schertler GF. The structural basis of agonist-induced activation in constitutively active rhodopsin. *Nature*. 2011; 471:656–660. [PubMed: 21389983]
27. Tesmer JJ. The quest to understand heterotrimeric G protein signaling. *Nat Struct Mol Biol*. 2010; 17:650–652. [PubMed: 20520658]
28. Fung BK, Hurley JB, Stryer L. Flow of information in the light-triggered cyclic nucleotide cascade of vision. *Proc Natl Acad Sci U S A*. 1981; 78:152–156. [PubMed: 6264430]
29. Bayburt TH, Leitz AJ, Xie G, Oprian DD, Sligar SG. Transducin activation by nanoscale lipid bilayers containing one and two rhodopsins. *J Biol Chem*. 2007; 282:14875–14881. [PubMed: 17395586]
30. Ernst OP, Gramse V, Kolbe M, Hofmann KP, Heck M. Monomeric G protein-coupled receptor rhodopsin in solution activates its G protein transducin at the diffusion limit. *Proc Natl Acad Sci U S A*. 2007; 104:10859–10864. [PubMed: 17578920]
31. Jastrzebska B, Goc A, Golczak M, Palczewski K. Phospholipids are needed for the proper formation, stability, and function of the photoactivated rhodopsin-transducin complex. *Biochemistry*. 2009; 48:5159–5170. [PubMed: 19413332]
32. Jastrzebska B, Golczak M, Fotiadis D, Engel A, Palczewski K. Isolation and functional characterization of a stable complex between photoactivated rhodopsin and the G protein, transducin. *Faseb J*. 2009; 23:371–381. [PubMed: 18827025]
33. Jastrzebska B, Tsybovsky Y, Palczewski K. Complexes between photoactivated rhodopsin and transducin: progress and questions. *Biochem J*. 2010; 428:1–10. [PubMed: 20423327]

34. Robinson PR, Cohen GB, Zhukovsky EA, Oprian DD. Constitutively active mutants of rhodopsin. *Neuron*. 1992; 9:719–725. [PubMed: 1356370]
35. Standfuss J, Zaitseva E, Mahalingam M, Vogel R. Structural impact of the E113Q counterion mutation on the activation and deactivation pathways of the G protein-coupled receptor rhodopsin. *J Mol Biol*. 2008; 380:145–157. [PubMed: 18511075]
36. Sakmar TP, Franke RR, Khorana HG. Glutamic acid-113 serves as the retinylidene Schiff base counterion in bovine rhodopsin. *Proc Natl Acad Sci U S A*. 1989; 86:8309–8313. [PubMed: 2573063]
37. Xie G, Gross AK, Oprian DD. An opsin mutant with increased thermal stability. *Biochemistry*. 2003; 42:1995–2001. [PubMed: 12590586]
38. Oprian DD, Molday RS, Kaufman RJ, Khorana HG. Expression of a synthetic bovine rhodopsin gene in monkey kidney cells. *Proc Natl Acad Sci U S A*. 1987; 84:8874–8878. [PubMed: 2962193]
39. Kaya AI, Thaker TM, Preininger AM, Iverson TM, Hamm HE. Coupling efficiency of rhodopsin and transducin in bicelles. *Biochemistry*. 2011; 50:3193–3203. [PubMed: 21375271]
40. McKibbin C, Farmer NA, Jeans C, Reeves PJ, Khorana HG, Wallace BA, Edwards PC, Villa C, Booth PJ. Opsin stability and folding: modulation by phospholipid bicelles. *J Mol Biol*. 2007; 374:1319–1332. [PubMed: 17996895]
41. MacKenzie D, Arendt A, Hargrave P, McDowell JH, Molday RS. Localization of binding sites for carboxyl terminal specific anti-rhodopsin monoclonal antibodies using synthetic peptides. *Biochemistry*. 1984; 23:6544–6549. [PubMed: 6529569]
42. Molday RS, MacKenzie D. Monoclonal antibodies to rhodopsin: characterization, cross-reactivity, and application as structural probes. *Biochemistry*. 1983; 22:653–660. [PubMed: 6188482]
43. Wessling-Resnick M, Johnson GL. Allosteric behavior in transducin activation mediated by rhodopsin. Initial rate analysis of guanine nucleotide exchange. *J Biol Chem*. 1987; 262:3697–3705. [PubMed: 3102494]
44. Lowry OH, Rosebrough NJ, Farr AL, Randall RJ. Protein measurement with the Folin phenol reagent. *J Biol Chem*. 1951; 193:265–275. [PubMed: 14907713]
45. Reeves PJ, Callewaert N, Contreras R, Khorana HG. Structure and function in rhodopsin: high-level expression of rhodopsin with restricted and homogeneous N-glycosylation by a tetracycline-inducible N-acetylglucosaminyltransferase I-negative HEK293S stable mammalian cell line. *Proc Natl Acad Sci U S A*. 2002; 99:13419–13424. [PubMed: 12370423]
46. Zhukovsky EA, Robinson PR, Oprian DD. Transducin activation by rhodopsin without a covalent bond to the 11-cis-retinal chromophore. *Science*. 1991; 251:558–560. [PubMed: 1990431]
47. Fasick JI, Lee N, Oprian DD. Spectral tuning in the human blue cone pigment. *Biochemistry*. 1999; 38:11593–11596. [PubMed: 10512613]
48. Edelhoch H. Spectroscopic determination of tryptophan and tyrosine in proteins. *Biochemistry*. 1967; 6:1948–1954. [PubMed: 6049437]
49. Pace CN, Vajdos F, Fee L, Grimsley G, Gray T. How to measure and predict the molar absorption coefficient of a protein. *Protein Sci*. 1995; 4:2411–2423. [PubMed: 8563639]
50. Molday RS, MacKenzie D. Inhibition of monoclonal antibody binding and proteolysis by light-induced phosphorylation of rhodopsin. *Biochemistry*. 1985; 24:776–781. [PubMed: 2581604]
51. Emeis D, Kuhn H, Reichert J, Hofmann KP. Complex formation between metarhodopsin II and GTP-binding protein in bovine photoreceptor membranes leads to a shift of the photoproduct equilibrium. *FEBS Lett*. 1982; 143:29–34. [PubMed: 6288450]
52. Bornancin F, Pfister C, Chabre M. The transitory complex between photoexcited rhodopsin and transducin. Reciprocal interaction between the retinal site in rhodopsin and the nucleotide site in transducin. *Eur J Biochem*. 1989; 184:687–698. [PubMed: 2509200]
53. Kuhn H, Bennett N, Michel-Villaz M, Chabre M. Interactions between photoexcited rhodopsin and GTP-binding protein: kinetic and stoichiometric analyses from light-scattering changes. *Proc Natl Acad Sci U S A*. 1981; 78:6873–6877. [PubMed: 6273893]
54. Kuhn H. Interactions Between Photoexcited Rhodopsin and Light-Activated Enzymes in Rods. *Progress in Retinal Research*. 1984; 3:123–156.

55. Banerjee S, Huber T, Sakmar TP. Rapid incorporation of functional rhodopsin into nanoscale apolipoprotein bound bilayer (NABB) particles. *J Mol Biol.* 2008; 377:1067–1081. [PubMed: 18313692]
56. Whorton MR, Jastrzebska B, Park PS, Fotiadis D, Engel A, Palczewski K, Sunahara RK. Efficient coupling of transducin to monomeric rhodopsin in a phospholipid bilayer. *J Biol Chem.* 2008; 283:4387–4394. [PubMed: 18033822]
57. Zhukovsky EA, Oprian DD. Effect of carboxylic acid side chains on the absorption maximum of visual pigments. *Science.* 1989; 246:928–930. [PubMed: 2573154]
58. Rasmussen SG, DeVree BT, Zou Y, Kruse AC, Chung KY, Kobilka TS, Thian FS, Chae PS, Pardon E, Calinski D, Mathiesen JM, Shah ST, Lyons JA, Caffrey M, Gellman SH, Steyaert J, Skinioitis G, Weis WI, Sunahara RK, Kobilka BK. Crystal structure of the  $\beta_2$  adrenergic receptor-Gs protein complex. *Nature.* 2011; 477:549–555. [PubMed: 21772288]

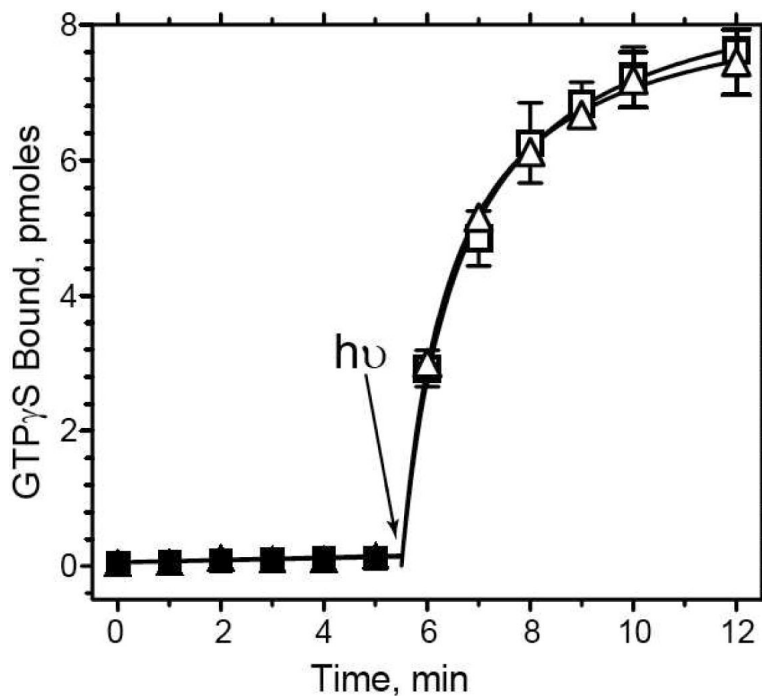


**Figure 1.** Effect of the 1D4 antibody on rhodopsin-catalyzed activation of transducin. Activation of transducin was monitored by following the binding of [ $^{35}$ S]-GTP $\gamma$ S with time in the presence (*squares*) and absence (*triangles*) of 1  $\mu$ M 1D4-antibody using a filter-binding assay as described in the Experimental Procedures. Each reaction contained 5 nM rhodopsin (N2C,E113Q,D282C mutant reconstituted with 11-cis-retinal), 1  $\mu$ M transducin and 3  $\mu$ M GTP $\gamma$ S, in 10 mM Tris buffer, pH 7.5, 100 mM NaCl, 5 mM MgCl $_2$ , 0.1 mM EDTA, and 0.01% DDM (w/v). Solid symbols, reaction in dark; open symbols, reaction after exposure to light (arrow). Error bars represent standard deviation ( $n = 2$ ). Some residual 1D4-peptide from the rhodopsin purification procedure was present but at concentrations at least 20-fold lower than the antibody combining sites.



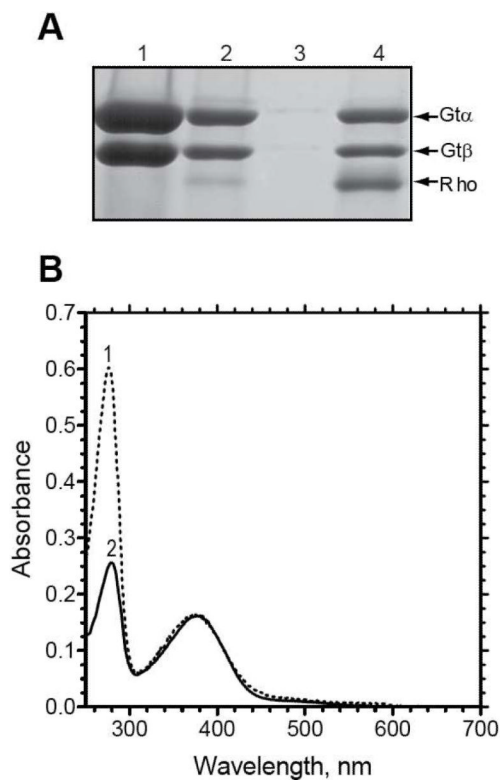


**Figure 2.**

Co-elution of transducin and rhodopsin from 1D4-Sepharose with 1D4-peptide. (A) SDS-PAGE analysis of various fractions from 1D4-immunoaffinity purification of the rhodopsin/transducin complex stained with Coomassie blue. *Lane 1*, transducin fraction applied to the immunoaffinity matrix; *lane 2*, unbound material; *lane 3*, last wash before elution of the complex; *lane 4*, fraction obtained upon elution with the 1D4-peptide. Only the  $\alpha$ - and  $\beta$ -subunits of transducin are shown. (B) UV/Visible absorption spectra of the N2C,E113Q,D282C mutant reconstituted with all-*trans*-retinal and purified by immunoaffinity chromatography on the 1D4-Sepharose matrix in the presence (*spectrum 1*) or absence (*spectrum 2*) of transducin.

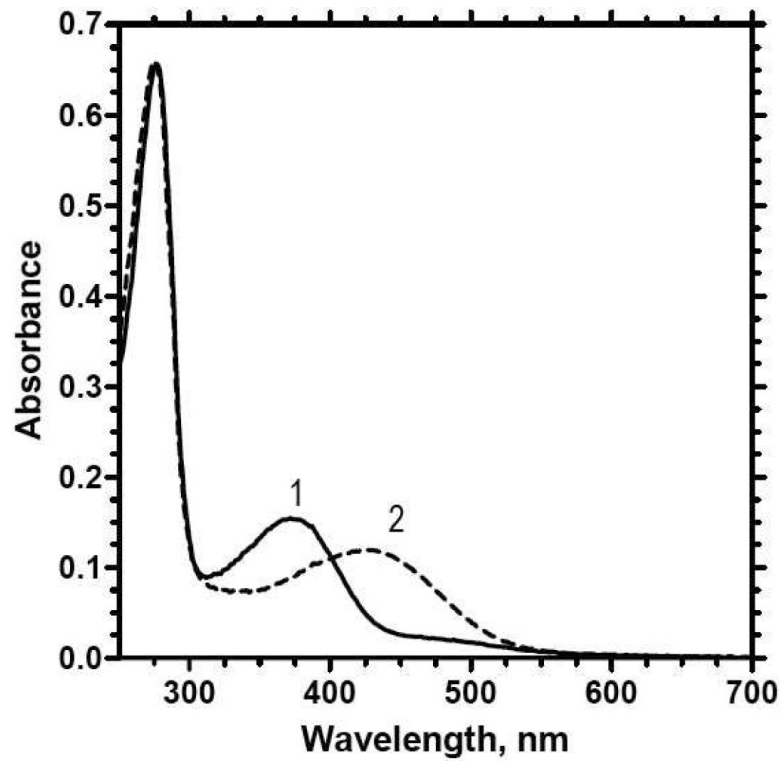


**Figure 3.** Determination of extinction coefficient at 380 nm for the retinal chromophore in the rhodopsin/transducin complex. *Spectrum 1* is that of the purified complex in 5 mM HEPES buffer, pH 7.5, containing 0.1 mM  $\text{MgCl}_2$  and 0.02% (w/v) DDM. *Spectrum 2* is that of the same sample immediately following addition of 50 mM sodium phosphate buffer, pH 3.5, and 0.5% SDS (final concentrations). *Spectrum 2* has been corrected for dilution.

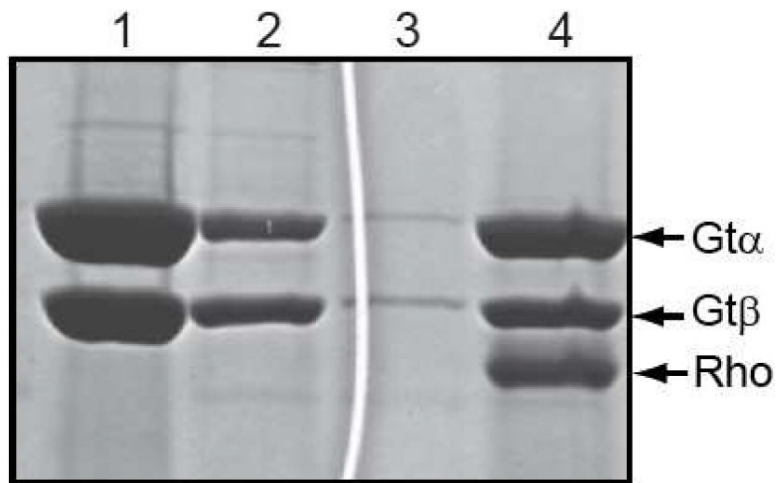


**Figure 4.** Co-elution of transducin and rhodopsin from ConA-Sepharose with  $\alpha$ -methylmannoside. SDS-PAGE analysis of various fractions from ConA-Sepharose affinity purification of the rhodopsin/transducin complex stained with Coomassie blue. *Lane 1*, transducin fraction applied to the ConA matrix; *lane 2*, unbound material; *lane 3*, last wash before elution of the complex; *lane 4*,  $\alpha$ -methylmannoside eluate. Only the  $\alpha$ - and  $\beta$ -subunits of transducin are shown.

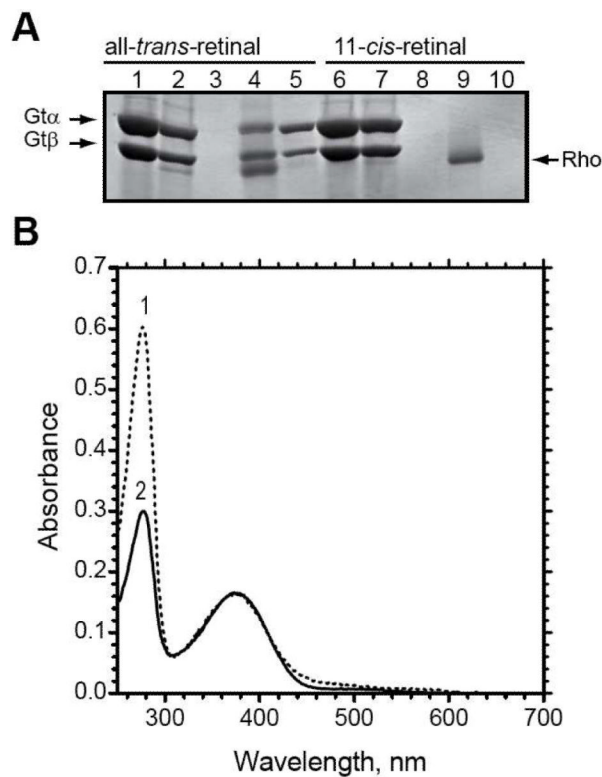


**Figure 5.**

The dependence of complex formation on activation of the N2C,E113Q,D282C mutant. (A) SDS-PAGE analysis of fractions from the purification of the rhodopsin N2C,E113Q,D282C mutant on 1D4-Sepharose in the presence of transducin, as visualized by Coomassie blue staining. The rhodopsin mutant was reconstituted with either *all-trans*-retinal (*lanes 1–5*) or *11-cis*-retinal (*lanes 5–10*), as is indicated in the figure. *Lanes 1 and 6*, transducin sample that was applied to the 1D4-matrix; *lanes 2 and 7*, unbound material; *lanes 3 and 8*, last wash; *lanes 4 and 9*, 1D4-peptide eluate; *lanes 5 and 10*, GTP $\gamma$ S eluate. Only the  $\alpha$ - and  $\beta$ -subunits of transducin are shown. (B) UV/Visible absorption spectra for the purified rhodopsin fractions. *Spectrum 1*, N2C,E113Q,D282C mutant reconstituted with *all-trans*-retinal (corresponding to fraction in A, *lane 4*); *spectrum 2*, N2C,E113Q,D282C mutant reconstituted with *11-cis*-retinal and purified in the dark (corresponding to fraction in A, *lane 9*).

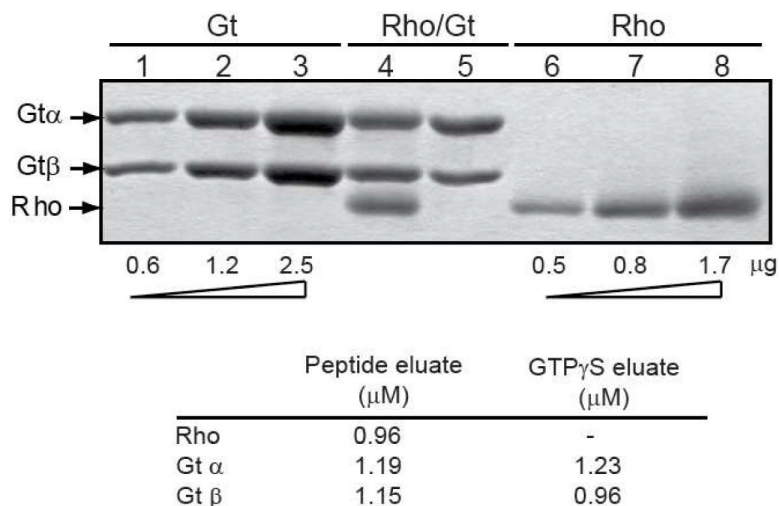


**Figure 6.** Densitometric determination of subunit stoichiometry in the activated rhodopsin/transducin complex. (A) SDS-PAGE analysis of the activated rhodopsin/transducin complex. *Lanes 1–3*, known standards of increasing amounts (as indicated) of purified transducin; *lanes 6–8*, known standards of increasing amounts (as indicated) of the N2C,E113Q,D282C mutant; *lane 4*, activated rhodopsin/transducin complex, purified on 1D4-Sepharose as in Figure 2; *lane 5*, GTP $\gamma$ S eluate from 1D4-Sepharose matrix. Only the  $\alpha$ - and  $\beta$ -subunits of transducin are shown. (B) Quantification of the complex subunits in A, *lanes 4 & 5* as determined by densitometry. Individual bands from SDS-PAGE gels were quantified as described in Experimental Procedures using ImageJ software and standard curves derived from known amounts of transducin and the rhodopsin N2C,E113Q,D282C mutant. The calculated concentration of released  $\beta$ -subunit in the GTP $\gamma$ S eluate suggests a fraction of this subunit is retained on the solid support.



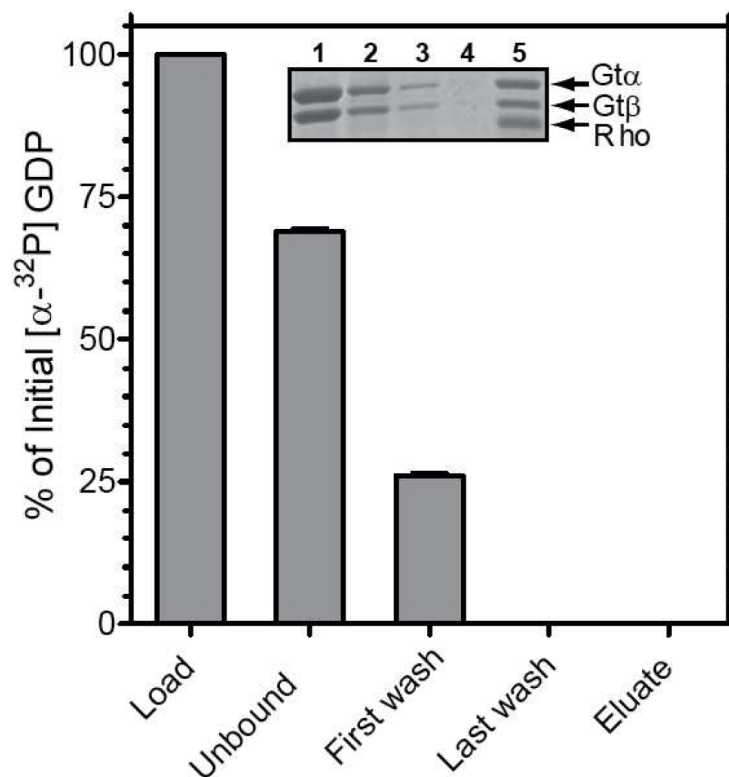


**Figure 7.** Nucleotide release during formation of the activated rhodopsin/transducin complex. The activated complex was formed on 1D4-Sepharose as described in Figure 2 using a transducin sample containing [ $\alpha$ - $^{32}$ P]-GDP in the nucleotide-binding pocket. Radioactivity in the fractions was monitored by liquid scintillation counting. Values are expressed as a percent of the total [ $\alpha$ - $^{32}$ P]-GDP in the loaded sample. Error bars represent standard deviation with  $n = 2$ . *Inset*, SDS-PAGE analysis of the steps in purification of the complex as visualized by Coomassie blue staining. *Lane 1*, transducin sample applied to the 1D4-matrix; *lane 2*, unbound fraction; *lane 3*, first wash; *lane 4*, last wash; *lane 5*, 1D4-peptide eluate. Note that the fraction in *lane 5* contains all components of the activated complex but no radioactivity.

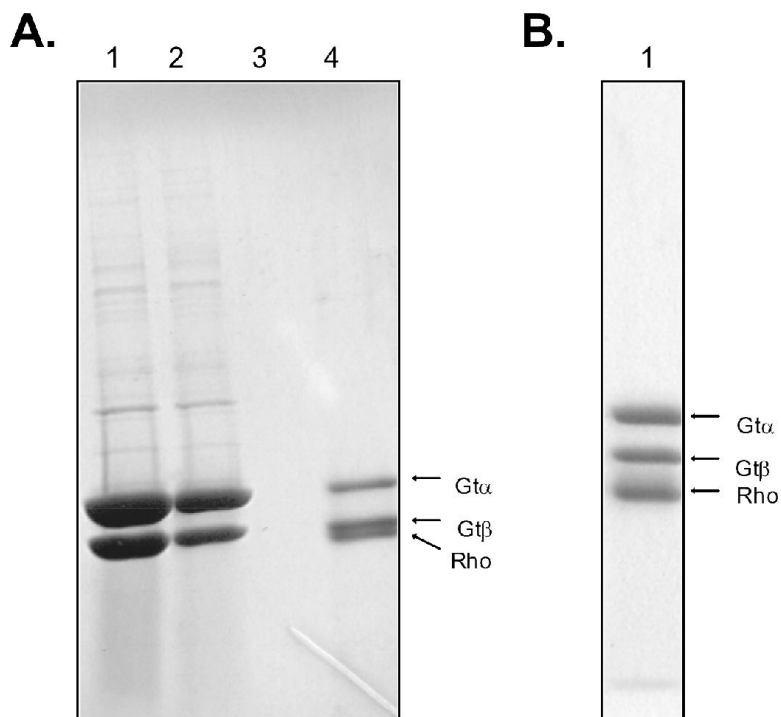


**Figure 8.** Purification of the complex using light activation of native and recombinant N2C,D282C rhodopsins. (A) SDS-PAGE analysis of various fractions from 1D4-immunoaffinity purification of the rhodopsin/transducin complex using light-activated native rhodopsin isolated from bovine retina. *Lane 1*, transducin fraction applied to the immunoaffinity matrix; *lane 2*, unbound material; *lane 3*, last wash before elution of the complex; *lane 4*, fraction obtained upon elution with the 1D4-peptide. (B) SDS-PAGE analysis of eluate from 1D4-column using light-activated recombinant N2C,D282C rhodopsin to form the complex. Only the  $\alpha$ - and  $\beta$ -subunits of transducin are shown in the gels. Note that native rhodopsin migrates more closely to the  $\beta$ -subunit of transducin than does the N2C,D282C mutant as a result of the mutant having one less oligosaccharyl chain (at position 2 in the sequence). Samples were activated by exposure to room lights for 2 minutes following addition of transducin to rhodopsin immobilized on the solid support. Bands in the gels were visualized by staining with Coomassie blue.

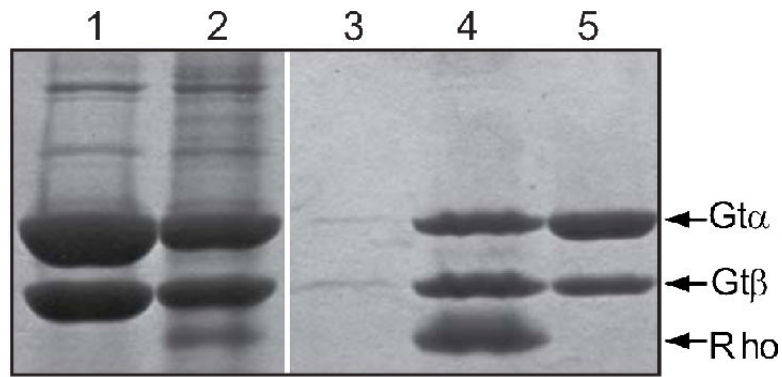


**Figure 9.** Purification of the activated rhodopsin/transducin complex in 2.5% DMPC/DHPC bicelles. The figure shows SDS-PAGE analysis of fractions from 1D4 immunoaffinity purification of the N2C,E113Q,D282C rhodopsin/transducin complex stained with Coomassie blue. The protocol was as described in Experimental Procedures using 2.5% DMPC/DHPC bicelles. *Lane 1*, transducin fraction applied to the column; *lane 2*, unbound material; *lane 3*, last wash before elution of the complex; *lane 4*, 1D4-peptide eluate; *lane 5*, GTP $\gamma$ S eluate. Only the  $\gamma$ - and  $\beta$ -subunits of transducin are shown. It should be noted here that in control experiments using buffers without bicelles no protein could be eluted from the immunoaffinity matrix with the 1D4-peptide.